# Mode Control in Photonic Crystal Vertical-Cavity Surface-Emitting Lasers and Coherent Arrays

Dominic F. Siriani, *Student Member, IEEE*, Meng Peun Tan, *Student Member, IEEE*, Ansas M. Kasten, *Student Member, IEEE*, Ann C. Lehman Harren, *Member, IEEE*, Paul O. Leisher, *Member, IEEE*, Joshua D. Sulkin, *Student Member, IEEE*, James J. Raftery, Jr., *Senior Member, IEEE*, Aaron J. Danner, *Member, IEEE*, Antonios V. Giannopoulos, *Student Member, IEEE*, and Kent D. Choquette, *Fellow, IEEE*

*(Invited Paper)*

***Abstract*—We demonstrate transverse mode control in vertical-cavity surface-emitting lasers (VCSELs) and 2-D VCSEL arrays. By etching a periodic arrangement of circular holes into the top distributed Bragg reflector mirror, we are able to control the lasing modes through index and loss confinement. Theoretical modeling of these confinement effects are shown to be consistent with experimental measurements. Photonic crystal etched patterns and ion-implanted photonic lattices have been employed to fabricate coherently-coupled 2-D arrays. Control of the array supermodes from the out-of-phase and in-phase conditions is discussed. Designs of photonic crystal coherent VCSEL arrays for high-power emission and beam steering applications are described.**

***Index Terms*—Distributed Bragg reflector (DBR) lasers, laser modes, semiconductor laser arrays, semiconductor lasers.**

## I. Introduction

VERTICAL-CAVITY surface-emitting lasers (VCSELs) are in widespread commercial use, particularly for short-range communication and position sensing. Their low-power consumption, low-cost and high-volume manufacturability, on-wafer testability, 2-D array configurability, and single longitudinal mode operation make VCSELs an appealing source over other semiconductor lasers. Despite these positive attributes, conventional VCSELs have disadvantages, especially concerning transverse mode control and single fundamental mode operation.

In order to design a single-mode VCSEL, a variety of transverse optical confinement approaches have been explored. These structures for mode control include oxide apertures [1], proton-implanted apertures [2], oxide/implant hybrid apertures [3], surface relief etched lasers [4], [5], photonic crystal patterns [6]–[11], and etched holey patterns [12], [13]. These approaches involve increasing the gain for the fundamental mode, increasing the loss of higher order modes, or properly designing the transverse refractive index profile to support only the lowest order mode. As a result, these methods require specific dimensions in their design (for example, cavity diameter, an etch depth, or oxide layer thickness), which can also often be correlated to the emission wavelength. In this paper, we focus on periodic photonic crystal patterns etched into the top distributed Bragg reflector (DBR) of VCSELs.

Photonic crystals, comprising a 2-D pattern in refractive index, have been shown to be useful for optical waveguiding in semiconductors and optical fiber [14]–[16]. In analyzing these waveguide structures, a photonic crystal with a missing hole, or defect, is treated as a step-index waveguide. It has been theoretically demonstrated that in photonic crystal fibers a photonic crystal can be used to achieve single-mode operation for an endless range of wavelengths [16]. This result led to the use of photonic crystals in VCSELs [6]–[11]. Although incapable of providing necessary current confinement, photonic crystal patterns etched into the top DBR of a VCSEL have been shown to provide good optical confinement to produce single-mode VCSELs.

In previous studies of oxide-confined, proton-implanted, and hybrid VCSELs, correlations have been made between the spectral mode characteristics and the induced refractive index contrast from the transverse confinement, where optical loss is neglected [17], [18]. However, recent studies of both optical fiber [19] and photonic crystal VCSELs [20], [21] have demonstrated that loss can have a significant effect on the cavity modes. Hence, to design efficient single-mode photonic crystal VCSELs requires an analysis that incorporates the effects on both the refractive index profile and the optical loss obtained from the photonic crystal.

2-D array configurations of photonic crystal VCSELs have also been investigated in the context of mode control. In

Manuscript received November 3, 2008; revised December 16, 2008. First published February 10, 2009; current version published June 5, 2009.

D. F. Siriani, M. P. Tan, A. M. Kasten, J. D. Sulkin, and A. V. Giannopoulos are with the Electrical and Computer Engineering Department, University of Illinois at Urbana-Champaign, Urbana, IL 61801 USA (e-mail: siriani@illinois.edu; mengtan@illinois.edu; akasten@illinois.edu; sulkin@illinois.edu; giannopo@illinois.edu).

A. C. Lehman Harren is with Sandia National Laboratories, Livermore, CA 94551 USA (e-mail: alehman@sandia.gov).

P. O. Leisher is with nLight Corporation, Vancouver, WA 98665 USA (e-mail: paul.leisher@nlight.net).

J. J. Raftery, Jr. is with the U.S. Military Academy, West Point, NY 10996 USA (e-mail: jim.raftery@us.army.mil).

A. J. Danner is with the Department of Electrical and Computer Engineering, National University of Singapore, Singapore 117576 (e-mail: adanner@nus.edu.sg).

K. D. Choquette is with the Electrical and Computer Engineering Department, University of Illinois at Urbana-Champaign, Urbana, IL 61801 USA (e-mail: choquett@illinois.edu).

Color versions of one or more of the figures in this paper are available online at http://ieeexplore.ieee.org.

Digital Object Identifier 10.1109/JSTQE.2008.2012121

particular, it is desirable in coherent VCSEL arrays to increase single-mode output and to control the far-field mode for beam steering. A large 2-D array of VCSELs can constitute a broad-area, high-power source with a narrow linewidth. Evanescent coupling between neighboring VCSELs will lock them together to operate on a single mode [22]–[32]. Through the optical coupling between adjacent VCSELs, an interference pattern can result in the far field. However, the observed supermode of 2-D VCSEL arrays is often found to be out-of-phase with several far-field peaks, rather than in-phase with a dominant on-axis far-field peak [24]. Manipulation of the phase relationship between coupled VCSELs can alter this interference pattern [26], and thus steer the location of the far-field intensity maximum [33]. Thus, the manipulation of modal properties of coherent arrays can enable several new applications for VCSELs.

The design, modeling, and properties of single-element photonic crystal VCSELs and coherent 2-D arrays are reviewed. A particular focus is the mechanisms and realization of mode control in photonic crystal VCSELs. The method of finding an effective refractive index for the photonic crystal VCSEL optical waveguide is reviewed, and this model is extended to include the effects of optical loss induced by the photonic crystal. Experimental results and comparisons with this theory are presented to characterize the operation of single-mode photonic crystal VCSELs. An overview of recent work on 2-D VCSEL arrays is also presented. The structures to achieve coherent coupling between adjacent VCSEL cavities are described. Our focus will be the analysis and manipulation of the coherently coupled supermodes formed in the array. In particular, the manipulation of phase in the array elements for the purposes of beam steering and control of the far-field mode will be presented. The initial prototypes of large, single-mode photonic crystal coherent VCSEL arrays are presented. The implications of mode control in VCSELs and 2-D VCSEL arrays through a variety of mechanisms will conclude this review.

## II. Photonic Crystal VCSEL Design

For single emitters, a photonic crystal VCSEL is a microcavity laser with a periodic pattern of air holes etched into the top DBR. Electrical confinement can be achieved using oxide confinement or ion implantation. A single or multiple missing-hole defect is located in the center of the photonic crystal pattern to create a transverse index-confinement structure. The oxide aperture or implant aperture is made larger than the photonic crystal defect aperture; in the implanted case, the optical effects of the thermal lens [34] formed in the operating laser are negligible since the thermal lens will be uniform across the photonic crystal aperture. Fig. 1 shows a cross section of an implanted photonic crystal VCSEL.

In this paper, the VCSEL epitaxial wafers have 20 or 22 top p-type DBR periods and 35 bottom n-type DBR periods with AlGaAs/GaAs quantum well active regions. Hexagonal arrays of circular holes etched into the top DBR are used as the photonic crystal and a single missing hole forms the laser cavity, as shown in Figs. 1 and 2 [6]–[11]. The array period $a$ and the hole diameter $b$ can be varied in order to investigate a

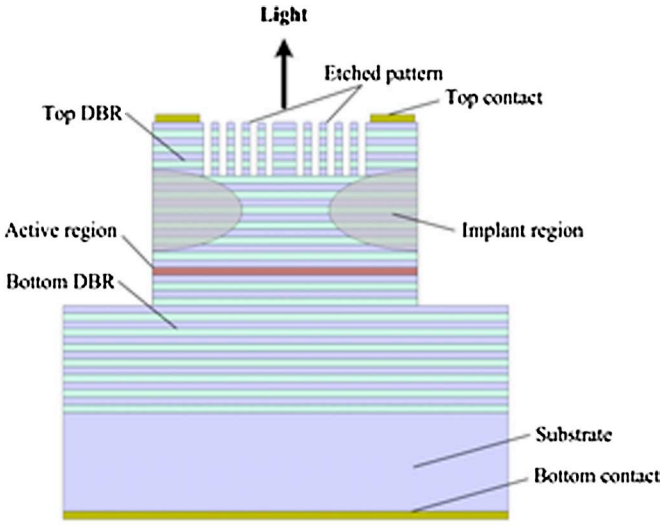


Fig. 1. Cross-sectional sketch of a photonic crystal VCSEL.

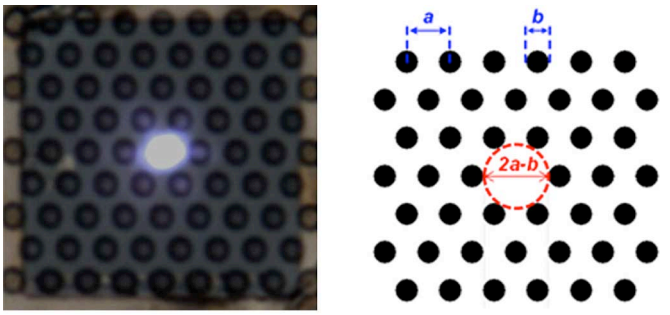


(a) (b)

Fig. 2. (a) Top view of a fabricated photonic crystal VCSEL while lasing and (b) sketch of the photonic crystal pattern etched into a VCSEL with parameters labeled.

wide range of structures. Altering $a$ and $b$ changes the effective refractive index of the photonic crystal as well as the diameter of the optical cavity, $2a$-$b$. We demonstrate that these alterations affect the waveguide formed by the photonic crystal and thus govern the modal properties of the VCSEL.

## III. Photonic Crystal VCSEL Modeling

Single-emitter photonic crystal VCSELs can be theoretically treated by using a simplified step-index optical fiber waveguide model. In this model, the defect in the photonic crystal is considered to be the core of the fiber, and the photonic crystal region surrounding is taken as the reduced-index cladding. The advantage of this approach is that it is less computationally intensive when compared to more rigorous methods such as finite-difference time-domain, finite element, or vectorial and 3-D calculations [35]–[37]. The purpose of the model we describe is to aid in the design of single-mode photonic crystal VCSELs.

The waveguiding and optical loss effects induced by the photonic crystal cladding are modeled using a complex refractive index. In order to find the real part of the effective refractive index of the photonic crystal cladding, the band diagram for the

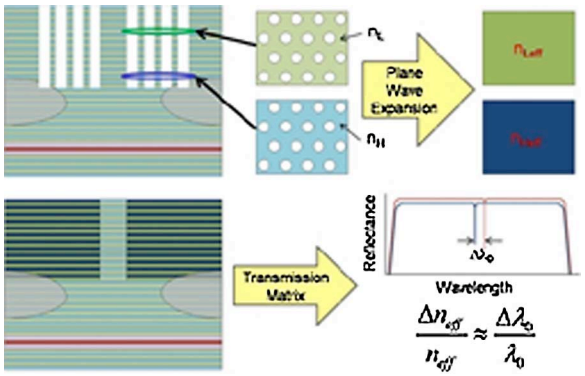


Fig. 3. Procedure used for finding the real part of the effective photonic crystal refractive index. Each individual high and low index layer penetrated by the photonic crystal is replaced with a layer with an effective index. These new values are inserted into a transfer matrix calculation to determine the index difference between the core and cladding regions.

photonic crystal in each DBR layer penetrated by the pattern is calculated using the plane wave expansion method. The photonic band diagram is needed since a geometric averaging of the semiconductor to air hole volume does not correctly determine the effective index [8]. The slope of the band for out-of-plane propagation $(k_z/k_0)$ can be used to find the effective refractive index. This effective index can then be used to replace the DBR layers penetrated by the photonic crystal with a homogeneous layer [9]. Using this information for the DBR, a 1-D transmission matrix approach can be used to calculate the resonance of both the core and cladding regions. The index step difference between these two regions can be found using the difference in the resonance wavelengths as given by [38]

$$\frac{\Delta n_{\text{eff}}}{n_{\text{eff}}} \approx \frac{\Delta \lambda_0}{\lambda_0} \tag{1}$$

where $n_{\text{eff}}$ is the effective refractive index of the core, $\lambda_0$ is the core resonance wavelength in free space, and $\Delta n_{\text{eff}}$ and $\Delta \lambda_0$ are the effective index and resonance wavelength differences, respectively. This procedure is schematically outlined in Fig. 3, and shows that the finite etch depth of the holes is intrinsically accounted for.

Having found an effective index for both the core and cladding regions of the photonic crystal VCSEL, it is then possible to solve the step-index fiber problem. To account for optical loss introduced by the finite-etch-depth holes, a complex refractive index is used for the cladding region [19]. Thus, the cladding index consists of a real part found by the procedure outlined earlier and an imaginary part

$$n_{\text{clad}} = n'_{\text{PhC}} + \text{i}n''_{\text{loss}}. \tag{2}$$

As discussed next, the imaginary index is found by fitting to the cold cavity spectral splitting between the first two optical modes.

The analysis is carried out by using finite differences in the frequency domain on the source-free scalar Helmholtz equation

$$\nabla^2 U + n^2(r) k_0^2 U = 0 \tag{3}$$

where $U$ is the field in three spatial dimensions, $n$ is the radial-dependent refractive index profile, and $k_0$ is the free space wave number. The problem is reduced to 1-D by assuming separable solutions of the form

$$U(r, \phi, z) = u(r) e^{-im\phi} e^{-ik_z z} \tag{4}$$

where $u$ is the radial field profile, $m$ is an integer, and $k_z$ is an effective propagation constant, which is assumed to be set by the optical length $(L)$ of the Fabry–Perot cavity created by the upper and lower DBRs

$$k_z = \frac{2\pi}{L}. \tag{5}$$

Inserting the solutions in (4) into the Helmholtz equation gives

$$\frac{d^2 u}{dr^2} + \frac{1}{r}\frac{du}{dr}\left(n^2(r)k_0^2 - k_z^2 - \frac{m^2}{r^2}\right) u(r) = 0 \tag{6}$$

Equation (6) then can be discretized using finite differences. This creates an eigenvalue problem with eigenvectors $u$ and eigenvalues $k_0$. Carrying out this analysis yields a set of solutions for the resonant modes of the waveguide whose wave numbers are $k_0$. The resonant wavelength is

$$\lambda_0 = \frac{2\pi c}{\text{Re}\{\omega_0\}} = \frac{2\pi}{\text{Re}\{k_0\}} \tag{7}$$

and the loss experienced by the mode is

$$\alpha_i = \text{Im}\{k_0\}. \tag{8}$$

This analysis can be compared to spectral data measured from fabricated photonic crystal VCSELs. The splitting in resonant wavelength between optical modes is sensitive to the loss in the cavity. This property is used to obtain the theoretical loss value by altering the imaginary part of the cladding refractive index such that the measured spectral splitting between the fundamental and first-order mode agrees with experiment [39].

## IV. Single-Mode Photonic Crystal VCSELs

Measurements from fabricated photonic crystal VCSELs are used to identify single-mode lasers designs. Threshold current for a particular photonic crystal VCSEL is found, and then the cold cavity spectrum is measured at a current lower than threshold (approximately 0.9 times threshold). Cold cavity spectra are measured to avoid spectral shifts arising from thermal effects. The optical loss induced by various photonic crystal patterns is determined by the spectral splitting between the fundamental and first higher order laser mode [39]. Fig. 4 shows a measured cold cavity spectrum with square points indicating the resonant wavelength values used in the theoretical analysis. The remaining circular points are the resulting calculated resonances. As can be seen in this figure, there is good agreement between the measured and calculated higher order mode resonances, and indicates the importance of including the effects of optical loss on the cavity confinement.

To determine the structure parameters for which photonic crystal VCSELs lase in a single-mode, cold cavity spectral measurements are taken on many photonic crystal VCSELs.

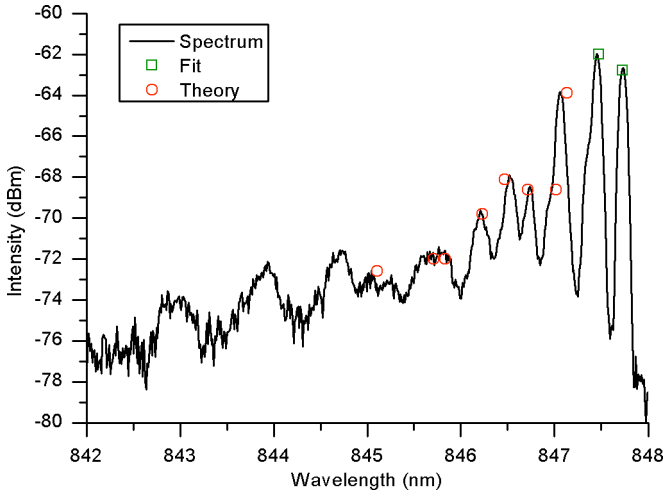


Fig. 4. Optical spectrum of a photonic crystal VCSEL showing fit points to the lowest two modes used for determining the loss (squares) and the solutions found for higher order modes using the lossy model (circles).

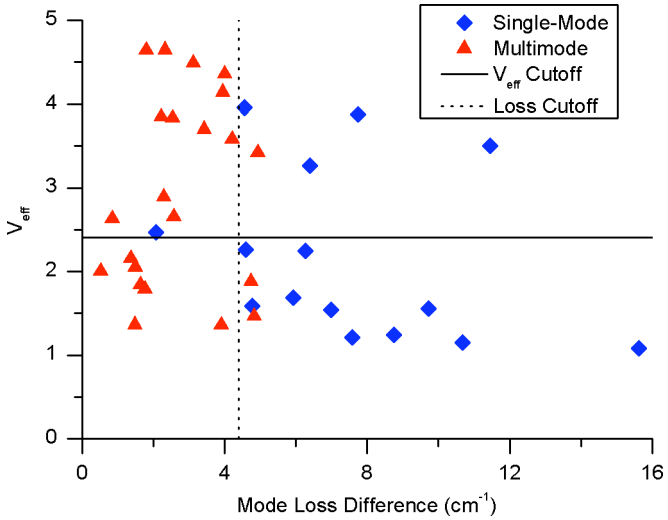


Fig. 5. Plot of the $V_{\text{eff}}$ parameter against the difference in loss between the fundamental and first higher order modes. The single-mode $V_{\text{eff}}$ cutoff is shown as a solid line and the apparent loss discrimination cutoff is shown as a dotted line.

The analysis described in Section III is then used to determine the loss for each design. Fig. 5 shows a summary of this investigation [21]. In this figure, the value of $V_{\text{eff}}$ calculated using a lossless analysis is plotted against the difference in loss between the first two modes calculated using the lossy analysis discussed earlier. As in conventional cylindrical fiber theory

$$V_{\text{eff}} = \frac{2\pi R}{\lambda}\sqrt{n_{\text{core}}^2 - n_{\text{clad}}^2} \tag{9}$$

where $R$ is the core radius and $\lambda$ is the free space optical wavelength. For a lossless guide, the single-mode cutoff is $V_{\text{eff}} < 2.405$, which is shown by a horizontal line in Fig. 5. It is clear that numerous multimode VCSELs operate below the cutoff and single-mode lasers operate above the cutoff. However, if optical loss is considered, a cutoff can be seen between

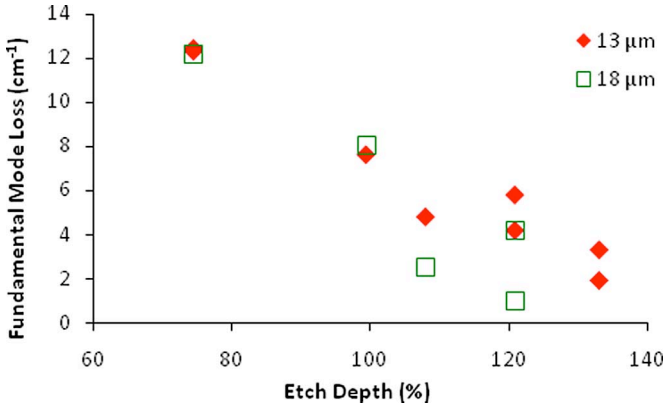


Fig. 6. Plot of the calculated fundamental mode loss against the measured etch depth in percent depth through the top DBR for single-mode photonic crystal VCSELs with $a = 4.0$ $\mu$m and $b/a = 0.7$.

single- and multimode lasing at approximately 5 cm$^{-1}$ of loss difference (dotted vertical line in Fig. 5). This mode discrimination is presumed to be the point at which the loss to higher order modes is too great for gain to compensate and thus lasing to occur.

In order to study the depth dependence of the photonic crystal design, a further study is performed on single-mode photonic crystal VCSELs. Multiple etch depths for a specific single photonic crystal design are investigated. The optical loss induced by the different hole etch depths is determined by the spectral splitting between the fundamental and first higher order mode. The lasers studied are oxide-confined VCSELs where the oxide aperture (13 and 18 $\mu$m diameters) is much larger than the defect aperture ($\sim 5$ $\mu$m diameter), so that the confinement and scattering effects of the oxide are negligible. Fig. 6 shows the measured optical loss following the aforementioned procedure plotted as a function of etch depth. It is apparent from this plot that an increased etch depth corresponds to a decrease in optical loss, even for hole depths penetrating into the bottom DBR. This can be explained by considering that the deeper etch will provide stronger mode confinement and thus reduce diffraction loss and scattering off the photonic crystal. It can also be observed that there is little difference in loss between the two different oxide aperture sizes, confirming that the oxide has negligible effect on the optical confinement and loss of the photonic crystal VCSELs.

## V. Coherent Photonic Crystal VCSEL Arrays

Coherently coupled 2-D arrays of VCSEL emitters have been fabricated using photonic crystal confinement [30]–[33] and active photonic crystal lattices [40]. Broad-area VCSELs have the advantage of sustaining higher output powers, but at the expense of supporting a large number of transverse modes. However, by using a collection of single-mode VCSELs in an array, it has been demonstrated that the lasers can couple together to form a single-array supermode [23], [24]. This coherently coupled single-mode array can be exploited in a variety of manners, for example, to reduce angular divergence, increase output power, and steer the far-field propagation direction.

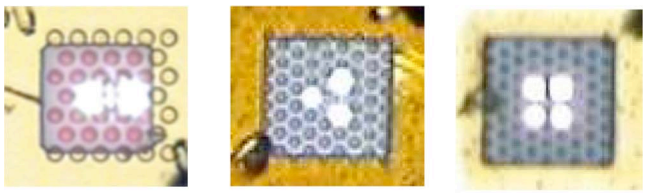

(a) (b) (c)

Fig. 7. Near-field image of (a) two-element, (b) three-element, and (c) four-element etched photonic crystal VCSEL arrays.

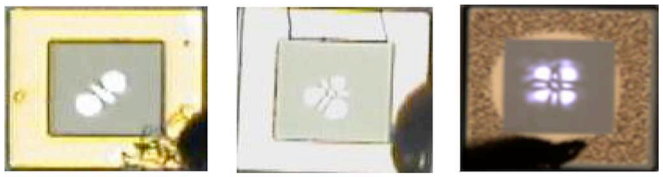

(a) (b) (c)

Fig. 8. Near-field images of ion-implanted photonic lattices with (a) two elements, (b) three elements, and (c) four elements.

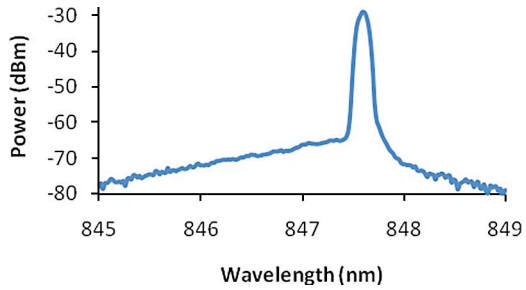


Fig. 9. Optical spectrum of a single-mode, two-by-one implanted VCSEL array.

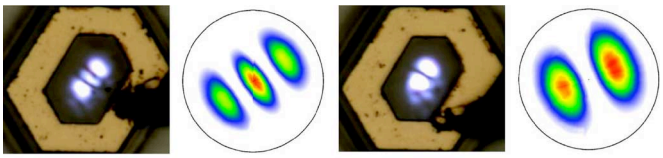

(a) (b)

Fig. 10. Near-field and far-field intensity images of two-by-one ion-implanted, two-element arrays operating (a) in phase and (b) out of phase.

Two configurations for coherent VCSEL arrays are explored in this paper, both of which exploit coupling between evanescent fields of adjacent cavities. The first is to use photonic crystal confinement (with an oxide aperture or ion implant current confinement) as described earlier with a pattern of multiple missing-hole defects. The multiple defects create an array of laser apertures. Adjacent lasing regions in the photonic crystal pattern can couple coherently through a gap or hole separating them. This coupling region can be specifically altered to change the coupling properties of the arrays (particularly phase and coupling strength) by varying the size and depth of the etched holes separating apertures. Fig. 7(a) shows a two-by-one array configuration with coupling through the center hole that has a smaller diameter [30]. Fig. 7(b) and (c) shows three- and four-element photonic crystal VCSEL arrays [31].

The other type of coherent 2-D VCSEL array is based on an active lattice of multiple implant apertures in a broad-area VCSEL [40]. In this design, the implant is used to provide both carrier and optical confinement. As with a typical implant-confined VCSEL, current confinement is provided by the crystal damage induced by ion implantation, while the optical confinement is provided by the gain and thermal lenses formed at the individual apertures [41]. In this manner, the multiple lasing elements constituting the 2-D array are created. Coupling between adjacent lasers in the array occurs in the implanted region separating apertures where there is a lower refractive index and/or gain. Fig. 8 shows examples of fabricated coherent implant arrays while lasing [40].

When coherently coupled, the VCSEL array tends to lase in only a single transverse mode. Fig. 9 shows a typical spectrum for a two-aperture photonic crystal array such as shown in Fig. 8(a). The lasing mode is generally the in-phase or out-of-phase coupled supermode [24]. For etched photonic crystal arrays, the lasing mode tends to be the out-of-phase mode, since presumably loss introduced by the etched hole separating the apertures favors the on-axis optical field null characteristic of the out-of-phase mode [31]. However, by reducing the size of the separating hole, it is possible to achieve in-phase lasing [32]. For implant arrays, the in-phase mode usually lases [40], which is attributed to the low loss between implant apertures. Examples of in-phase and out-of-phase near- and far-field intensities for two-by-one implant arrays are shown in Fig. 10.

In 2-D VCSEL arrays, mode manipulation can be performed. Specifically, it is possible to influence the properties of the individual, separated VCSEL cavities to modify the properties of the coupled supermode. In fact, by altering the cavity properties, the VCSEL array can change from lasing on one coupled supermode to lasing on multiple individual cavity modes (i.e., the elements of the array can become spectrally decoupled). The simplest way to individually modify the cavities is through current injection. By separating the top contacts on the VCSEL device (using individual contacts separated by more than a micrometer, or by physically removing material between the contacts), one can nominally inject current selectively to a particular VCSEL aperture while minimally affecting adjacent cavities. The cavity refractive index thus can be altered though current-induced refractive index changes, which result in a change of cavity resonance [33]. In changing the resonances between cavities, one also changes the phase and coherence relationship between them [42].

An application of phase tuning between cavities is far-field beam steering. By changing the relative phase between cavities, the location of the far-field intensity maximum is altered [33]. Using three VCSEL elements, steering in 2-D has been achieved [43]. For example, by separating the top contact using a focused ion beam etch, each VCSEL element can be individually controlled. Fig. 11 shows the top facet of a three-element VCSEL array defined by implantation, where a focused ion beam etch through the contact layers of the upper DBR approximately electrically isolates the three elements. The different images in Fig. 11 correspond to current injection into the

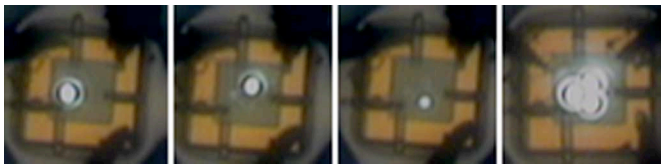

Fig. 11. Near-field images of a three-element implant array with segmented contacts and coherent operation of all elements.

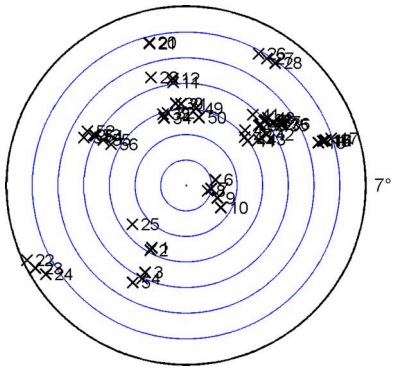


Fig. 12. Map of the angular location of the far-field intensity maximum for different current injection schemes into a three-element array.

individual elements or simultaneously to all three elements of the array. These images illustrate that the contact separation is sufficient for addressable control of the lasers. Fig. 12 is a map of the angular location of the far-field maximum for a variety of current injection schemes to the separated contacts. Each cross in Fig. 12 corresponds to a unique combination of the three injection currents into the array. Far-field simulations show there is not a unique set of phases that correspond to a specific far field. The beam steering in Fig. 12 is limited by the onset of higher order modes, leading to incomplete far-field coverage. The onset of multiple modes reduces the coherence and eliminates the interference pattern that makes steering possible. Moreover, the thermally induced optical confinement provided by the implantation will also permit decoupling of the lasers when they are driven at different current injections. This demonstrates that using selective current injection has the potential of controlling the far-field mode of a coherent VCSEL array for beam steering applications.

Single-mode lasers with increased power can also be achieved using coherent VCSEL arrays. A large number of VCSELs can be coupled together to create a single, large supermode, which ideally operates in the in-phase mode. Increased power results from the broad-area lasing, but a single mode is maintained as a result of the coherent locking of the VCSELs. We have demonstrated a ninefold increase in output power in a four-by-four photonic crystal coherent array shown in Fig. 13. In Fig. 14(a), a dominant peak in the optical spectrum can be seen for this laser array, and the far field shown in Fig. 14(b) exhibits a high degree of coherence [42]. This indicates the array is coupled; however, the far field also shows an on-axis null, which is indicative of out-of-phase operation. Ideally, single-mode in-phase lasing is desired, and thus the ion-implanted photonic lattice VCSEL arrays may be promising for this application.

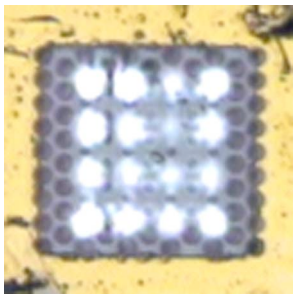

Fig. 13. Near-field image of a four-by-four photonic crystal VCSEL array.

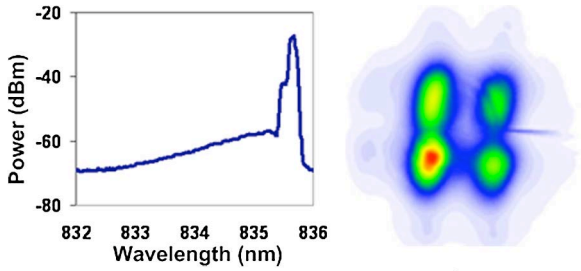


Fig. 14. (a) Optical spectrum and (b) out-of-phase far-field intensity of the four-by-four photonic crystal VCSEL array.

## VI. Conclusion

Transverse mode control has been extensively studied for photonic crystal VCSELs and VCSEL arrays. A lossy model for the photonic crystal waveguide used for transverse confinement in VCSELs has been developed. This model has been demonstrated to design single-mode VCSELs with increased efficiency and output power. In VCSEL arrays, control of the array supermode has been investigated and exploited for several applications. In-phase and out-of-phase far-field modes have been obtained in both photonic crystal and ion-implanted arrays. Manipulation of these modes has been demonstrated to be useful for beam steering and increased single-mode output power. Ongoing research focuses on theoretically investigating the coherence properties and coupling mechanisms of VCSEL arrays. Moreover, etched photonic crystals combined with implant-confined arrays are being pursued to gain the described benefits of these two designs.

These developments in the control of transverse modes can significantly advance the use of VCSELs for a number of applications. With the methods developed here, photonic crystal VCSELs can be designed to operate only on a single mode while maintaining a larger aperture size and higher efficiency. Thus, these advancements could enable a single-mode VCSEL with high output powers and greater reliability for sensing and long-haul communication applications. The demonstrated supermode coupling in VCSEL arrays has shown potential for creating single-mode, large-area, high-power VCSELs for similar applications. The manipulation of such supermodes has also been shown useful for beam steering, which could be used for laser scanning and sensing applications as well as optical switching in reconfigurable photonic systems. Thus, by controlling the

modal properties in VCSELs and 2-D VCSEL arrays through the use of photonic crystals, the versatility and functionality of these laser sources are enhanced.

## REFERENCES


[1] C. Jung, R. Jager, M. Grabherr, P. Schnitzer, R. Michalzik, B. Weigl, S. Muller, and K. J. Ebeling, "4.8 mW single-mode oxide confined top-surface emitting vertical-cavity laser diodes," *Electron. Lett.*, vol. 33, no. 21, pp. 1790–1791, 1997.

[2] R. A. Morgan, G. D. Guth, M. W. Focht, M. T. Asom, K. Kojima, L. E. Rogers, and S. E. Callis, "Transverse mode control of vertical-cavity top-surface-emitting lasers," *IEEE Photon. Technol. Lett.*, vol. 4, no. 4, pp. 374–377, Apr. 1993.

[3] E. W. Young, K. D. Choquette, S. L. Chuang, K. M. Geib, A. J. Fischer, and A. A. Allerman, "Single-transverse-mode vertical-cavity lasers under continuous and pulsed operation," *IEEE Photon. Technol. Lett.*, vol. 13, no. 9, pp. 927–929, Sep. 2001.

[4] H. Martinsson, J. A. Vukusic, M. Grabherr, R. Michalzik, R. Jager, K. J. Ebeling, and A. Larsson, "Transverse mode selection in large-area oxide-confined vertical-cavity surface-emitting lasers using a shallow surface relief," *IEEE Photon. Technol. Lett.*, vol. 11, no. 12, pp. 1536–1538, Dec. 1999.

[5] H. J. Unold, S. W. Z. Mahmoud, R. Jager, M. Kicherer, M. C. Riedl, and K. J. Ebeling, "Improving single-mode VCSEL performance by introducing a long monolithic cavity," *IEEE Photon. Technol. Lett.*, vol. 12, no. 8, pp. 939–941, Aug. 2000.

[6] D. S. Song, S. H. Kim, H. G. Park, C. K. Kim, and Y. H. Lee, "Single-fundamental-mode photonic-crystal vertical-cavity surface- emitting lasers," *Appl. Phys. Lett.*, vol. 80, pp. 3901–3903, 2002.

[7] N. Yokouchi, A. J. Danner, and K. D. Choquette, "Two-dimensional photonic crystal confined vertical-cavity surface-emitting lasers," *IEEE J. Sel. Topics Quantum Electron.*, vol. 9, no. 5, pp. 1439–1445, Sep./Oct. 2003.

[8] N. Yokouchi, A. J. Danner, and K. D. Choquette, "Etching depth dependence of the effective refractive index in two-dimensional photonic-crystal-patterned vertical-cavity surface-emitting laser structures," *Appl. Phys. Lett.*, vol. 82, no. 9, pp. 1344–1346, 2003.

[9] A. J. Danner, J. J. Raftery, Jr., T. Kim, P. O. Leisher, A. V. Giannopoulos, and K. D. Choquette, "Progress in photonic crystal vertical cavity lasers," *IEICE Trans. Electron.*, vol. E88-C, no. 5, pp. 944–950, 2005.

[10] A. J. Danner, T. S. Kim, and K. D. Choquette, "Single fundamental mode photonic crystal vertical cavity laser with improved output power," *Electron. Lett.*, vol. 41, no. 6, pp. 325–326, 2005.

[11] H. P. D. Yang, F. I. Lai, Y. H. Chang, H. C. Yu, C. P. Sung, H. C. Kuo, S. C. Wang, S. Y. Lin, and J. Y. Chi, "Singlemode (SMSR $>$ 40 dB) proton-implanted photonic crystal vertical-cavity surface emitting lasers," *Electron. Lett.*, vol. 41, no. 6, pp. 326–328, 2005.

[12] A. Furukawa, S. Sasaki, M. Hoshi, A. Matsuzono, K. Moritoh, and T. Baba, "High-power single-mode vertical-cavity surface-emitting lasers with triangular holey structure," *Appl. Phys. Lett.*, vol. 85, pp. 5161–5163, 2004.

[13] P. O. Leisher, A. J. Danner, J. J. Raftery, Jr., and K. D. Choquette, "Proton implanted single mode holey vertical-cavity surface emitting lasers," *Electron. Lett.*, vol. 41, no. 18, pp. 1010–1011, 2005.

[14] A. Mekis, J. C. Chen, I. Kurland, S. Fan, P. R. Villeneuve, and J. D. Joannopoulos, "High transmission through sharp bends in photonic crystal waveguides," *Phys. Rev. Lett.*, vol. 77, no. 18, pp. 3787–3790, 1996.

[15] J. C. Knight, T. A. Birks, P. S. J. Russell, and D. M. Atkin, "All-silica single-mode fiber with photonic crystal cladding," *Opt. Lett.*, vol. 21, no. 19, pp. 1547–1549, Oct. 1996.

[16] T. A. Birks, J. C. Knight, and P. S. J. Russell, "Endlessly single-mode photonic crystal fiber," *Opt. Lett.*, vol. 22, no. 13, pp. 961–963, 1997.

[17] K. L. Lear, K. D. Choquette, R. P. Schneider, Jr., and S. P. Kilcoyne, "Modal analysis of a small surface emitting laser with a selectively oxidized waveguide," *Appl. Phys. Lett.*, vol. 66, no. 20, pp. 2616–2618, 1995.

[18] E. W. Young, K. D. Choquette, J.-F. P. Seurin, S. L. Chuang, K. M. Geib, and A. A. Allerman, "Comparison of wavelength splitting for selectively oxidized, ion implanted, and hybrid vertical-cavity surface-emitting lasers," *IEEE J. Quantum Electron.*, vol. 39, no. 5, pp. 634–639, May 2003.

[19] A. E. Siegman, "Propagating modes in gain-guided optical fibers," *J. Opt. Soc. Amer. A*, vol. 20, no. 8, pp. 1617–1628, 2003.

[20] K.-H. Lee, J.-H. Baek, I.-K. Hwang, and Y.-H. Lee, "Square-lattice photonic-crystal vertical-cavity surface-emitting lasers," *Opt. Express*, vol. 12, no. 17, pp. 4136–4143, 2004.

[21] D. F. Siriani, P. O. Leisher, and K. D. Choquette, "Loss-induced confinement in photonic crystal vertical-cavity surface-emitting lasers," in *Proc. IEEE LEOS Meeting*, 2007, pp. 630–631.

[22] H.-J. Yoo, A. Scherer, J. P. Harbison, L. T. Florez, E. G. Paek, B. P. V. der Gaag, J. R. Hayes, A. V. Lehman, E. Kapon, and Y.-S. Kwon, "Fabrication of a two-dimensional phased array of vertical-cavity surface-emitting lasers," *Appl. Phys. Lett.*, vol. 56, no. 13, pp. 1198–1200, 1990.

[23] H.-J. Yoo, J. R. Hayes, E. G. Paek, A. Scherer, and Y.-S. Kwon, "Array mode analysis of two-dimension phased arrays of vertical cavity surface emitting lasers," *IEEE J. Quantum Electron.*, vol. 26, no. 6, pp. 1039–1051, Jun. 1990.

[24] G. R. Hadley, "Modes of a two-dimensional phase-locked array of vertical-cavity surface-emitting lasers," *Opt. Lett.*, vol. 15, no. 21, pp. 1215–1217, 1990.

[25] P. L. Gourley, M. E. Warren, G. R. Hadley, G. A. Vawter, T. M. Brennan, and B. E. Hammons, "Coherent beams from high efficiency two-dimensional surface-emitting semiconductor laser arrays," *Appl. Phys. Lett.*, vol. 58, no. 9, pp. 890–892, 1991.

[26] M. E. Warren, P. L. Gourley, G. R. Hadley, G. A. Vawter, T. M. Brennan, B. E. Hammons, and K. L. Lear, "On-axis far-field emission from two-dimensional phase-locked vertical-cavity surface-emitting laser arrays with an integrated phase-corrector," *Appl. Phys. Lett.*, vol. 61, no. 13, pp. 1484–1486, 1992.

[27] M. Orenstein, E. Kapon, J. P. Harbison, L. T. Florez, and N. G. Stoffel, "Large two-dimensional arrays of phase-locked vertical cavity surface emitting lasers," *Appl. Phys. Lett.*, vol. 60, no. 13, pp. 1535–1537, 1992.

[28] R. A. Morgan, K. Kojima, T. Mullally, G. D. Guth, M. W. Focht, R. E. Leibenguth, and M. Asom, "High-power coherently coupled $8\times8$ vertical cavity surface emitting laser array," *Appl. Phys. Lett.*, vol. 61, no. 10, pp. 1160–1162, 1992.

[29] R. M. di Sopra, M. Brunner, H.-P. Gauggel, H. P. Zappe, M. Moser, R. Hovel, and E. Kapon, "Continuous-wave operation of phase-coupled vertical-cavity surface-emitting laser arrays," *Appl. Phys. Lett.*, vol. 77, no. 15, pp. 2283–2285, 2000.

[30] A. J. Danner, J. C. Lee, J. J. Raftery, Jr., N. Yokouchi, and K. D. Choquette, "Coupled-defect photonic crystal vertical cavity surface emitting lasers," *Electron. Lett.*, vol. 39, no. 18, pp. 1323–1324, 2003.

[31] J. J. Raftery, Jr., A. J. Danner, J. C. Lee, and K. D. Choquette, "Coherent coupling of two-dimensional arrays of defect cavities in photonic crystal vertical cavity surface-emitting lasers," *Appl. Phys. Lett.*, vol. 86, no. 20, pp. 201104-1–201104-3, 2005.

[32] J. J. Raftery, Jr., A. C. Lehman, A. J. Danner, P. O. Leisher, A. V. Giannopoulos, and K. D. Choquette, "In-phase evanescent coupling of two-dimensional arrays of defect cavities in photonic crystal vertical cavity surface emitting lasers," *Appl. Phys. Lett.*, vol. 89, pp. 081119-1–081119-3, 2006.

[33] A. C. Lehman, J. J. Raftery, Jr., A. J. Danner, P. O. Leisher, and K. D. Choquette, "Relative phase tuning of coupled defects in photonic crystal vertical-cavity surface-emitting lasers," *Appl. Phys. Lett.*, vol. 88, pp. 021102-1–021102-2, 2006.

[34] N. K. Dutta, L. W. Tu, G. Hasnain, G. Zydzik, Y. H. Wang, and A. Y. Cho, "Anomalous temporal response of gain guided surface emitting lasers," *Electron. Lett.*, vol. 27, no. 3, pp. 208–210, 1991.

[35] P. Bienstman, R. Baets, J. Vukusic, A. Larsson, M. J. Noble, M. Brunner, K. Gulden, P. Debernardi, L. Fratta, G. P. Bava, H. Wenzel, B. Klein, O. Conradi, R. Pregla, S. A. Riyopoulos, J.-F. P. Seurin, and S. L. Chuang, "Comparison of optical VCSEL models on the simulation of oxide-confined devices," *IEEE J. Quantum Electron.*, vol. 37, no. 12, pp. 1618–1631, Dec. 2001.

[36] T. Czyszanowski, M. Dems, and K. Panajotov, "Single mode condition and modes discrimination in photonic-crystal 1.3 $\mu$m AlInGaAs/InP VCSEL," *Opt. Express*, vol. 15, no. 9, pp. 5604–5608, 2007.

[37] T. Czyszanowski, M. Dems, and K. Panajotov, "Optimal parameters of photonic crystal vertical-cavity surface-emitting diode lasers," *IEEE J. Lightw. Technol.*, vol. 25, no. 9, pp. 2331–2336, Sep. 2007.

[38] G. R. Hadley, "Effective index model for vertical-cavity surface-emitting lasers," *Opt. Lett.*, vol. 20, no. 13, pp. 1483–1485, 1995.

[39] D. F. Siriani, P. O. Leisher, and K. D. Choquette, "Loss induced confinement in photonic crystal vertical cavity surface emitting lasers," *IEEE J. Quantum Electron.*, to be published.
[40] A. C. Lehman and K. D. Choquette, "One- and two-dimensional coherently coupled implant-defined vertical-cavity laser arrays," *IEEE Photon. Technol. Lett.*, vol. 19, no. 19, pp. 1421–1423, Oct. 2007.
[41] K. D. Choquette and K. M. Geib, "Fabrication and performance of vertical-cavity surface-emitting lasers," in *Vertical-Cavity Surface-Emitting Lasers*, C. W. Wilmsen, H. Temkin, and L. A. Coldren, Eds. New York: Cambridge, 1999, pp. 193–232.
[42] A. C. Lehman, J. J. Raftery, Jr., P. S. Carney, and K. D. Choquette, "Coherence of Photonic Crystal Vertical-Cavity Surface-Emitting Laser Arrays," *IEEE J. Quantum Electron.*, vol. 43, no. 1, pp. 25–30, Jan. 2007.
[43] A. C. Lehman, D. F. Siriani, and K. D. Choquette, "Two-dimensional electronic beam-steering with implant-defined coherent VCSEL arrays," *Electron. Lett.*, vol. 43, no. 22, pp. 1202–1203, 2007.

**Dominic F. Siriani** (S'07) received the B.S. and M.S. degrees in electrical engineering in 2006 and 2007, respectively, from the University of Illinois at Urbana-Champaign, Urbana-Champaign, where he is currently working toward the Ph.D. degree.

His current research interests include photonic crystal vertical-cavity surface-emitting lasers (VCSELs) and VCSEL arrays.

Mr. Siriani is a Student Member of the IEEE/Lasers and Electro-Optics Society. He is a National Science Foundation (NSF) Graduate Fellow and a National Defense Science and Engineering Graduate (NDSEG) Fellow.

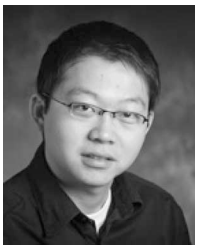

**Meng Peun Tan** (S'08) received the B.S. degree in electrical engineering in 2007 from the University of Illinois at Urbana-Champaign, Urbana-Champaign, where he is currently working toward the M.S. degree in electrical engineering.

His current research interests include microstructured active photonic devices such as photonic crystal vertical-cavity surface-emitting lasers (VCSELs).

Mr. Tan is a Student Member of the IEEE/Lasers and Electro-Optics Society.

**Ansas M. Kasten** (S'07) received the Diploma in electrical engineering from the University of the Saarland, Saarbrücken, Germany, in 2003, and the M.S. degree in electrical engineering in 2006 from the University of Illinois at Urbana-Champaign, Urbana-Champaign, where he is currently working toward the Ph.D. degree at the Department of Electrical and Computer Engineering.

From 2003 to 2004, he was a Visiting Scholar in the Department of Agricultural Engineering, University of Illinois, where he later joined the Photonics Device Research Group. His current research interests include photonic devices such as vertical-cavity surface-emitting lasers (VCSELs), VCSEL arrays, detector arrays, photonic crystal VCSELs, and their integration into microfluidic systems for biomedical sensing applications.

Mr. Kasten is a Student Member of the Optical Society of America (OSA).

**Ann C. Lehman Harren** (S'03–M'04) received the B.S., M.S., and Ph.D. degrees in electrical engineering from the University of Illinois at Urbana-Champaign, Urbana-Champaign, in 2002, 2004, and 2007, respectively.

She is currently with Sandia National Laboratories, Livermore, CA. Her current research interests include novel photonic sources and detectors.

Dr. Harren is a member of the IEEE/Lasers and Electro-Optics Society.

**Paul O. Leisher** (S'98–M'07) received the B.S. degree in electrical engineering from Bradley University, Peoria, IL, in 2002, and the M.S. and Ph.D. degrees in electrical and computer engineering from the University of Illinois at Urbana-Champaign, Urbana-Champaign, in 2004 and 2007, respectively.

In 2007, he joined nLight Corporation, Vancouver, WA, where he is currently a Device Engineer. He has authored more than 60 technical journal articles and conference presentations. His current research interests include the design, fabrication, characterization, and analysis of semiconductor lasers and other photonic devices.

Dr. Leisher is a member of the IEEE Lasers and Electro-Optics Society and the Optical Society of America (OSA).

**Joshua D. Sulkin** (S'02) received the B.S. degree in computer engineering in 2006 from the University of Illinois, Urbana-Champaign, where he is currently working toward the M.S. degree in electrical engineering.

He joined the Photonic Device Research Group as an Undergraduate Research Assistant affiliated with the Center for Nanoscale Chemical-Electrical-Mechanical Systems. His current research interests include photonic devices such as vertical-cavity surface-emitting lasers, and their integration with microfluidic networks for sensing and manufacturing applications.

**James J. Raftery, Jr.** (S'94–M'95–SM'06) received the B.S. degree from Washington University in St. Louis, St. Louis, MO, the M.S. degree from the University of Missouri—Columbia, Columbia, in 1996, and the Ph.D. degree from the University of Illinois at Urbana-Champaign, Urbana-Champaign, in 2005, all in electrical engineering.

He was commissioned as an officer in the United States Army in 1988. In 1996, he joined the Faculty of the Department of Electrical Engineering and Computer Science at the United States Military Academy (USMA), West Point, NY. In 1999, he became the Power and Energy Research Program Manager at the Army Research Laboratory, Adelphi, MD. In 2001, he assumed duties as the Assistant Project Manager for Soldier Power at Fort Belvoir, VA. In 2005, he returned to the Electrical Engineering Faculty at USMA. In 2007, he was chartered as a Product Manager (PM) within the Army's Program Executive Office for Intelligence, Electronic Warfare, and Sensors at Ft. Monmouth, NJ. His current research interests include photonic crystal vertical-cavity surface-emitting lasers.

Dr. Raftery is a Senior Member of the IEEE/Lasers and Electro-Optics Society (LEOS), and a member of the Optical Society of America (OSA) and the American Society for Engineering Education (ASEE).

**Aaron J. Danner** (S'98–M'05) received the B.S. degree in electrical engineering from the University of Missouri—Columbia, Columbia, and the M.S. and Ph.D. degrees from the University of Illinois—Urbana-Champaign, Urbana-Champaign.

In 2006, he joined the Electrical Engineering Faculty at the National University of Singapore.

Dr. Danner is a member of the IEEE/Lasers and Electro-Optics Society (LEOS) and the Optical Society of America (OSA).

**Antonios V. Giannopoulos** (S'06) recieved the B.S. degrees in electrical engineering and mathematics in 2003 and the M.S. degree in electrical engineering from the University of Illinois at Urbana-Champaign, Urbana-Champaign, where he is working toward the Ph.D. degree and is currently a member of the Photonics Device Research Group.

His current research interests include design, fabrication, and testing of 2-D photonic crystal membrane lasers and nanophotonic devices.

Mr. Giannopoulos is a Student Member of the IEEE/Lasers and Electro-Optics Society.

**Kent D. Choquette** (M'97–SM'02–F'03) received the B.S. degrees in engineering physics and applied mathematics from the University of Colorado—Boulder, Boulder, and the M.S. and Ph.D. degrees in materials science from the University of Wisconsin—Madison, Madison.

From 1990 to 1992, he was a Postdoctoral Researcher at AT&T Bell Laboratories, Murray Hill, NJ. He then joined Sandia National Laboratories, Albuquerque, NM, and from 1993 to 2000 was a Principal Member of Technical Staff. He became a Professor in the Electrical and Computer Engineering Department at the University of Illinois at Urbana-Champaign, Urbana-Champaign, in 2000. He has authored more than 200 technical publications and three book chapters, and has presented numerous invited talks and tutorials.

Prof. Choquette is a Fellow of the Optical Society of America (OSA) and The International Society for Optical Engineering (SPIE). He served as an Associate Editor of the IEEE JOURNAL OF QUANTUM ELECTRONICS and the IEEE PHOTONIC TECHNOLOGY LETTERS, and as a Guest Editor of the IEEE JOURNAL OF SELECTED TOPICS IN QUANTUM ELECTRONICS. From 2000 to 2002, he was an IEEE/Lasers and Electro-Optics Society (LEOS) Distinguished Lecturer. He was the recipient of the 2008 IEEE/LEOS Engineering Achievement Award.